Accepted Manuscript

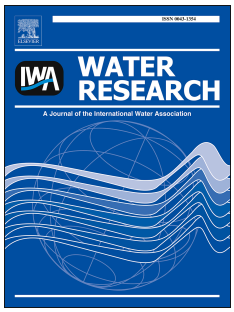

Modelling anaerobic co-digestion in Benchmark Simulation Model No. 2: parameter estimation, substrate characterisation and plant-wide integration

Magnus Arnell, Sergi Astals, Linda Åmand, Damien J. Batstone, Paul D. Jensen, Ulf Jeppsson

PII: S0043-1354(16)30195-6

DOI: 10.1016/j.watres.2016.03.070

Reference: WR 11954

To appear in: *Water Research*

Received Date: 5 January 2016

Revised Date: 30 March 2016

Accepted Date: 31 March 2016

Please cite this article as: Arnell, M., Astals, S., Åmand, L., Batstone, D.J., Jensen, P.D., Jeppsson, U., Modelling anaerobic co-digestion in Benchmark Simulation Model No. 2: parameter estimation, substrate characterisation and plant-wide integration, *Water Research* (2016), doi: 10.1016/j.watres.2016.03.070.

This is a PDF file of an unedited manuscript that has been accepted for publication. As a service to our customers we are providing this early version of the manuscript. The manuscript will undergo copyediting, typesetting, and review of the resulting proof before it is published in its final form. Please note that during the production process errors may be discovered which could affect the content, and all legal disclaimers that apply to the journal pertain.

ACCEPTED MANUSCRIPT

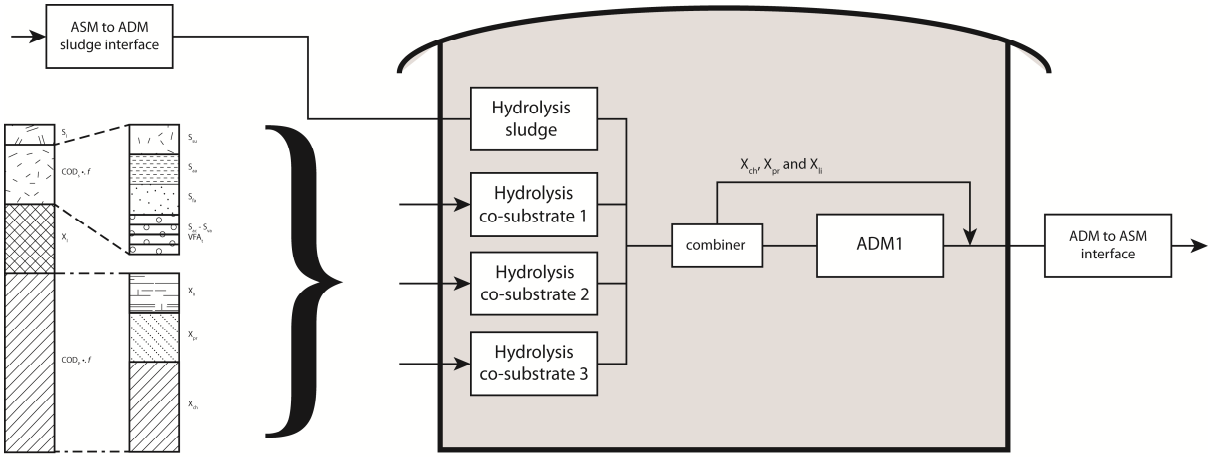

ACCEPTED MANUS

ACCEPTED MANUSCRIPT

Modelling anaerobic co-digestion in Benchmark Simulation Model No. 2: parameter estimation, substrate characterisation and plant-wide integration

Magnus Arnell[a,b], Sergi Astals[c], Linda Åmand[d], Damien J. Batstone[c], Paul D. Jensen[c], Ulf Jeppsson[a]

[a] Department of Biomedical Engineering (BME), Division of Industrial Electrical Engineering and Automation (IEA), Lund University, P.O. Box 118, SE-221 00 Lund, Sweden. (E-mail: magnus.arnell@iea.lth.se; ulf.jeppsson@iea.lth.se)

[b] SP Technical Research Institute of Sweden, Gjuterigatan 1D, SE-582 73 Linköping, Sweden.

[c] Advanced Water Management Centre, The University of Queensland, Brisbane, QLD 4072, Australia. (E-mail: s.astals@awmc.uq.edu.au; d.batstone@awmc.uq.edu.au; p.jensen@awmc.uq.edu.au)

[d] IVL Swedish Environmental Research Institute, P.O. Box 210 60, SE-100 31, Stockholm, Sweden. (E-mail: linda.amand@ivl.se)

Corresponding author: Magnus Arnell, E-mail: magnus.arnell@iea.lth.se, Phone: +46 (0)10 516 63 33, Fax: +46 (0)46 142114.

Abstract

Anaerobic co-digestion is an emerging practice at wastewater treatment plants (WWTPs) to improve the energy balance and integrate waste management. Modelling of co-digestion in a plant-wide WWTP model is a powerful tool to assess the impact of co-substrate selection and dose strategy on digester performance and plant-wide effects. A feasible procedure to characterise and fractionate co-substrates COD for the Benchmark Simulation Model No. 2 (BSM2) was developed. This procedure is

ACCEPTED MANUSCRIPT

also applicable for the Anaerobic Digestion Model No. 1 (ADM1). Long chain fatty acid inhibition was included in the ADM1 model to allow for realistic modelling of lipid rich co-substrates. Sensitivity analysis revealed that, apart from the biodegradable fraction of COD, protein and lipid fractions are the most important fractions for methane production and digester stability, with at least two major failure modes identified through principal component analysis (PCA). The model and procedure were tested on biochemical methane potential (BMP) tests on three substrates, each rich on carbohydrates, proteins or lipids with good predictive capability in all three cases. This model was then applied to a plant-wide simulation study which confirmed the positive effects of co-digestion on methane production and total operational cost. Simulations also revealed the importance of limiting the protein load to the anaerobic digester to avoid ammonia inhibition in the digester and overloading of the nitrogen removal processes in the water train. In contrast, the digester can treat relatively high loads of lipid rich substrates without prolonged disturbances.

Keywords: Mathematical modelling; ADM1; Anaerobic digestion; LCFA inhibition; Waste characterisation; Codigestion.

GRAPHICAL ABSTRACT

Separate figure file attached.

HIGHLIGHTS

- Practical methodology for co-substrate characterization and fractionation for ADM1
- Key components of co-substrate feed identified by sensitivity analysis
- Implementation of anaerobic co-digestion in BSM2 and a supporting case study
- Plant-wide effects of co-substrate selection and feed strategy demonstrated

Nomenclature

AcoD	Anaerobic co-digestion
AD	Anaerobic digestion
ADM1	Anaerobic Digestion Model No. 1
ASM	Activated Sludge Model
ASM1	Activated Sludge Model No. 1
ASU	Activated sludge unit
B_0	Ultimate methane potential [m^3 CH_4.ton VS^{-1}]
BMP	Biomethane potential
BOD	Biological oxygen demand [kg O_2.m^{-3}]
BSM2	Benchmark Simulation Model No. 2
C_i	Concentration of substance *i* [kg.m^{-3}]
COD	Chemical oxygen demand [kg O_2.m^{-3}]
COD_P	Particulate fraction of chemical oxygen demand [kg O_2.m^{-3}]
COD_s	Soluble fraction of chemical oxygen demand [kg O_2.m^{-3}]
COD_t	Total chemical oxygen demand [kg O_2.m^{-3}]
DAF	Dissolved air flotation
DO	Dissolved oxygen [kg O_2.m^{-3}]
EQI	Effluent quality index
f_d	Biodegradable fraction of total chemical oxygen demand [-]
γ_i	Conversion factor to COD for substance *i* (kg COD.kg^{-1}).
GISCOD	General Integrated Solid Waste Co-Digestion model
I_{fa}	Long chain fatty acids inhibition (ADM1) [-]
I_{NH}	Ammonia inhibition (ASM1) [-]
ISS	Inorganic suspended solids
$K_{I,50}$	50% inhibitory concentration (ADM1) [kg COD.m^{-3}.d^{-1}]
$K_{i,fa,low}$	Parameter in long chain fatty acid inhibition (ADM1)

$K_{i,fa,high}$	Parameter in long chain fatty acid inhibition (ADM1)
k_{hyd}	Hydrolysis parameter (ADM1) [d^{-1}]
$k_{hyd,sludge}$	Hydrolysis parameter for sludge (ADM1) [d^{-1}]
LCFA	Long chain fatty acids
M_N	Molar mass of nitrogen [$g.mol^{-1}$]
NOx-N	Total nitrate and nitrite nitrogen [kg $N.m^{-3}$]
OCI	Operational cost index
OLR_{ext}	Organic loading rate for co-substrates [kg $COD.m^{-3}.d^{-1}$]
OLR_{sludge}	Organic loading rate for sludge [kg $COD.m^{-3}.d^{-1}$]
PCA	Principal component analysis
$pH_{LL,ac}$	Lower limit of pH inhibition of uptake of acetate (ADM1)
Q_{gas}	Flow of biogas [$m^3.d^{-1}$]
Q_{CH4}	Flow of biomethane [m^3 $CH_4.d^{-1}$]
S_{aa}	Amino acids (ADM1) [kg $COD.m^{-3}$]
S_{ac}	Total acetic acid (ADM1) [kg $COD.m^{-3}$]
S_{bu}	Total butyric acid (ADM1) [kg $COD.m^{-3}$]
S_{fa}	Fatty acids (ADM1) [kg $COD.m^{-3}$]
S_I	Inert soluble organics (ADM1) [kg $COD.m^{-3}$]
S_{IN}	Inorganic nitrogen (ADM1) ($kmol.m^{-3}$)
S_{pro}	Total propionic acid (ADM1) [kg $COD.m^{-3}$]
S_{su}	Sugars (ADM1) [kg $COD.m^{-3}$]
S_{va}	Total valeric acid (ADM1) [kg $COD.m^{-3}$]
TAN	Total ammonia nitrogen [kg $N.m^{-3}$]
TKN	Total Kjeldahl nitrogen [kg $N.m^{-3}$]
TN	Total nitrogen [kg $N.m^{-3}$]
TS	Total solids [$kg.m^{-3}$]
TSS	Total suspended solids [$kg.m^{-3}$]

ACCEPTED MANUSCRIPT

VFA	Volatile fatty acids [kg.m^{-3}]
VFA_t	Total volatile fatty acids [kg.m^{-3}]
VS	Volatile solids [kg.m^{-3}]
WWTP	Wastewater treatment plant
X_c	Composite material (ADM1) [kg COD.m^{-3}]
X_{ch}	Carbohydrates (ADM1) [kg COD.m^{-3}]
X_i	Inert particulate organics (ADM1) [kg COD.m^{-3}]
X_{li}	Lipids (ADM1) [kg COD.m^{-3}]
X_{pr}	Proteins (ADM1) [kg COD.m^{-3}]

1 Introduction

The scope for wastewater treatment plants (WWTPs) has widened during recent years. Not only are the discharge limits getting stricter, also new constraints such as resource recovery, energy efficiency and mitigation of greenhouse gas emissions are being applied (Olsson, 2015). These issues increase the focus on energy recovery by anaerobic digestion (AD) at WWTPs. Many full-scale anaerobic digesters are oversized and therefore under-utilised (Lundkvist, 2005). Anaerobic co-digestion (AcoD) of organic wastes with sewage sludge allows the WWTPs to use residual digester capacity and thereby increase methane production and subsequently energy production (Batstone and Virdis, 2014, Mata-Alvarez *et al*., 2014). The application of AcoD at WWTPs is becoming more common and in the future is it likely that most medium to large size plants will practice AcoD. Even though the co-substrates are fed directly to the digester and not to the WWTP influent, it still produces an additional load on the WWTP water train. The organic matter in the co-substrate is degraded to a certain extent in the AD process and converted to biogas; however, mineralized nutrients are mobilised and recirculated to the water train. Therefore, one of the key factors for succeeding with AcoD is to select suitable co-substrate/s and their optimal dose rate. Co-substrate characteristics and applicability have been extensively reviewed by Mata-Alvarez *et al*. (2014). Ideal co-substrates will have a high methane

potential, high degradable fraction (and minimum impact on residual solids production) and a nutrient composition suitably balanced for the host WWTP. Generally, this means that co-substrate characteristics will differ from those of WWTP sludges in terms of composition and degradation kinetics. While there are a large number of potential co-substrates suitable for treatment at WWTP, local substrate availability and transport costs will constrain the options for individual plants. Effective modelling of AcoD is a powerful tool to assess the resource efficiency, energy balance and plant-wide effects of various co-substrate feeds at a WWTP (Razaviarani and Buchanan, 2015).

To compare the performance of different control strategies in a unified framework the Benchmark Simulation Model No. 2 (BSM2) was developed (Gernaey *et al.*, 2014). BSM2 represents a plant-wide model including digestion of sludge with the Anaerobic Digestion Model No. 1 (ADM1, Batstone *et al.*, 2002). In light of the increased focus on digestion, it is important that the AD process is well described and allows modelling of common and developing applications, such as AcoD. However, the current standard implementation of ADM1 in BSM2 does not allow for addition of co-substrates or dynamic hydrolysis parameters. Furthermore, some important limitations in the AD related to AcoD common practice in WWTP are missing, such as long chain fatty acid (LCFA) inhibition. The major variation in co-substrates composition poses a challenge for modelling AcoD since the model parameters have to be calibrated accordingly; and for dynamic simulations and evaluation of operational strategies, flexibility in feed composition is necessary since it also can vary over time. In the literature there are several examples of how to modify ADM1 for such purposes. The simplest approach is to characterise the actual feed mix. Derbal *et al.* (2009) uses the standard procedure from Batstone *et al.* (2002) to acquire the stoichiometric composition of composite particulate chemical oxygen demand (COD) (X_c), i.e. carbohydrates (X_{ch}), proteins (X_{pr}), lipids (X_{li}) and inerts (X_I). This approach is successful in terms of model predictions but leads to an inflexible model since the substrate mix cannot be varied without repeating the characterisation. Esposito *et al.* (2008) modelled AcoD of sewage sludge and food waste using a modified ADM1. For the degradation of particulate organic matter they used the standard formulation of ADM1 with disintegration and hydrolysis for all substrates and biomass decay. In order to separate the different streams they used multiple pools of

composite material, i.e. X_{c1} , X_{c2}, etc. each with its individual disintegration kinetics. A more general and flexible method for applying AcoD with ADM1 is the General Integrated Solid Waste Co-Digestion model (GISCOD) presented by Zaher *et al.* (2009). In the GISCOD model the particulate feed substrate is characterized as X_{ch}, X_{pr}, X_{li} and X_I, and using X_c only for internal biomass decay, i.e. X_c will only consist of dead biomass. To keep the hydrolysis for different substrates apart the GISCOD model virtually separates the hydrolysis model from the remaining processes of ADM1. This makes the model easy to expand for an arbitrary number of substrates, and flexible enough to allow for dynamic simulations with a variable mix of substrates in the digester feed. The main disadvantage is the large number of parameters and states needed where multiple complex substrates are fed, though it is common that for a given substrate, a common hydrolysis parameter for carbohydrates, lipids and proteins will be used. The interface approach used in the BSM2 (Nopens *et al*., 2009) also applies this approach, fractionating all particulate substrates to carbohydrates, proteins and lipids. Indeed, there is a general recommendation to avoid the use of the X_c variable for input characterisation due to inflexibility in input characterisation (Batstone *et al*., 2015).

One of the most important aspects for a successful modelling project is feed characterisation (including feed fractionation) and estimation of substrate dependent parameters. Several methods for feed fractionation have been suggested in literature (Kleerebezem and van Loosdrecht, 2006; Lübken *et al.*, 2007; Zaher *et al*., 2009; Wichern *et al.*, 2009; Nopens *et al*., 2009; Girault *et al*., 2012; Astals *et al.*, 2013; Jimenez *et al*., 2015). While some of these methods are comprehensive and provide a detailed feed characterisation, they are also complicated and include analyses and methods not commonly performed in AD testing. The problem of input characterisation remains a major challenge as identified in a key recent review of AD modelling, particularly for mixed digesters (Batstone *et al*., 2015). The feasibility of a characterisation method for engineering purposes is determined by simplicity, transparency, affordability and fit for purpose accuracy. Therefore, the analyses used must be (if not already routine), common, robust, applicable on most substrates and affordable. The resulting model feed composition must at the same time be accurate enough to assure model predictive

capability for relevant outputs, such as gas production, volatile solids (VS) destruction and digestate composition.

This paper investigates the influence of the substrate characteristics on model outputs and proposes a comprehensive method for implementing AcoD in a plant-wide WWTP model including:

- characterisation of substrates;
- estimation of the substrate dependent parameters;
- modifications of ADM1; and
- integration of AcoD in a plant-wide model structure, i.e. BSM2.

A simulation study is presented with three co-substrates, each rich on carbohydrates, proteins or lipids, to assess the plant-wide effects of AcoD on WWTPs.

2 Materials and Methods

2.1 Input model

An input model was developed to apply AcoD in BSM2 and plant-wide models in general. The input model is divided in two steps:

Step 1 – a method to estimate the biodegradable part of COD (f_d) (or methane potential B_0 – these are fully correlated, see below), and the substrate dependent model parameters, i.e. the hydrolysis parameters (k_{hyd}) for particulate matter from biomethane potential (BMP) tests.

Step 2 – using the estimated f_d and basic physio-chemical data on the co-substrate, a scheme for fractionation of COD and total nitrogen (TN) into the classification of ADM1 state variables is proposed. The selection of important input co-substrate variables (out of the 26 default ADM1 state variables listed in the Supplementary information, Table S.1) was determined by the sensitivity analysis described in Section 2.5.

In the first step the ultimate methane potential (B_0) and k_{hyd} are estimated by fitting a model to BMP data. Fitting a first-order function with a non-linear optimization routine is known to be a straight

forward option (Arnell and Åmand, 2014; Jensen *et al*., 2011; Angelidaki *et al.*, 2009). The full ADM1 model can also be used to model the BMP test with a similar optimization routine (but more complex model). In both cases the sum of squared errors should be used as objective function (Arnell and Åmand, 2014; Jensen *et al*., 2011). For this study both options were evaluated, but only results from the full ADM1 BMP model are presented below since the simple first-order model was inappropriate when inhibition was present (e.g., fatty feed). The value of f_d is determined from the B_0 estimate according to Eq. (1).

$$f_{\mathrm{d}} = \frac{B_0}{350\ \mathrm{COD_t}}\mathrm{VS} \quad (1)$$

where:

B_0 is the ultimate methane potential [$Nm^3\ CH_4.ton\ VS^{-1}$];

COD_t is the total COD [$kg\ COD.m^{-3}$];

f_d is the biodegradable part of COD_t [-]; and

VS is the volatile solids [$kg.m^{-3}$].

The schematic fractionation for the second step is illustrated in Figure 1. The particulate and soluble inert state variables are set as products of f_d and the respective particulate and soluble COD, Eqs. (2) and (3). The ADM1 does not consider inorganic suspended solids (ISS). That means that the contribution by the ash content of the substrates is not included. For modelling of substrates with high TS/VS ratio the model should be expanded with ISS as a non-reactive particulate state variable.

Figure 1. Scheme for fractionation of COD into the most influential state variables of ADM1. Corresponding equation number in parenthesis.

$$S_{\mathrm{I}} = \mathrm{COD_s}(1 - f_{\mathrm{d}}) \quad (2)$$

$$X_{\mathrm{I}} = \mathrm{COD_p}\,(1 - f_{\mathrm{d}}) \quad (3)$$

where:

COD_s is the soluble COD [kg COD.m^{-3}];

COD_p is the particulate COD [kg COD.m^{-3}].

Secondly, the particulate biodegradable COD is considered. The variables X_{pr} and X_{li} are calculated from measurements converted to COD (conversion factors given in Supplementary information, Table S.2), Eqs. (4) and (5), and the remaining part assigned to X_{ch}, Eq. (6). This strategy, previously also suggested by Galí *et al.* (2009), is chosen since proteins and lipids generally are easier to analyse than carbohydrates for solid substrates, and leaving enough degrees of freedom to close the mass balance. The biodegradability of the respective fractions is assumed equal to the overall degradability, f_d.

$$X_{li} = C_{li}\,\gamma_{li}\,f_d \quad (4)$$

$$X_{pr} = C_{pr}\,\gamma_{pr}\,f_d \quad (5)$$

$$X_{ch} = COD_p\,f_d - X_{pr} - X_{li} \quad (6)$$

where:

C_i is the concentration of substance i [kg.m^{-3}];

γ_i is the conversion factor to COD for substance i [kg COD.kg^{-1}]. Values given in Supplementary information, Table S.2.

The four VFA state variables can be calculated directly by converting the measured values to COD, Eqs. (7) to (10). Assuming the soluble COD is small the state variables S_{su}, S_{aa} and S_{fa} can be split equal to their corresponding particulates, Eqs. (11) to (13). This assumption is better than just neglecting these state variables or splitting them in thirds as suggested by Astals *et al.* (2013) since it is based on available data. However, for substrates with a high proportion of COD_S, $> 10\%$, the soluble fractions need greater attention. Measurements of carbohydrate, protein and lipid contents of COD_S are then recommended.

$$S_{\mathrm{ac}} = C_{\mathrm{Ac}}\,\gamma_{\mathrm{Ac}} \quad (7)$$

$$S_{\mathrm{pro}} = C_{\mathrm{pro}}\,\gamma_{\mathrm{pro}} \quad (8)$$

$$S_{\mathrm{bu}} = C_{\mathrm{bu}}\,\gamma_{\mathrm{bu}} \quad (9)$$

$$S_{\mathrm{va}} = C_{\mathrm{va}}\,\gamma_{\mathrm{va}} \quad (10)$$

$$S_{\mathrm{su}} = (\mathrm{COD_s}\,f_{\mathrm{d}} - \mathrm{VFA_t})\frac{X_{\mathrm{ch}}}{\mathrm{COD_p}\,f_{\mathrm{d}}} \quad (11)$$

$$S_{aa} = (\mathrm{COD_s}\,f_{\mathrm{d}} - \mathrm{VFA_t})\frac{X_{\mathrm{pr}}}{\mathrm{COD_p}\,f_{\mathrm{d}}} \quad (12)$$

$$S_{\mathrm{fa}} = (\mathrm{COD_s}\,f_{\mathrm{d}} - \mathrm{VFA_t})\frac{X_{\mathrm{li}}}{\mathrm{COD_p}\,f_{\mathrm{d}}} \quad (13)$$

where:

$\mathrm{VFA_t}$ is the sum of all VFAs [kg COD.m^{-3}].

The soluble inorganic nitrogen content S_{IN} is calculated from the total ammonia nitrogen (TAN) by Eq. (14). For this study, the remaining state variables of the ADM1 were set to 0. If the substrate has a non-neutral pH the acid-base balances must be considered (Batstone *et al.*, 2002). Furthermore, for other special substrates, for example rich on alcohols such as ethanol, methanol or glycerol, special fractionation schemes and model modifications may be needed (García-Gen *et al*., 2013).

$$S_{\mathrm{IN}} = \frac{\mathrm{TAN}}{M_N 1000} \quad (14)$$

where:

TAN is the total ammonia nitrogen [g N.m^{-3}];

M_N is the molar mass of nitrogen [g.mol^{-1}].

The data requirements to follow the above fractionation scheme are: TS, VS, $\mathrm{COD_t}$, $\mathrm{COD_s}$, VFAs (i.e. Acetate, Propionate, Butyrate and Valerate), Proteins, Lipids, TAN and a BMP test.

2.2 ADM1 modifications

The initial simulations for the sensitivity analysis (see Sections 2.5 and 3.3) using the default BSM2 implementation of ADM1 showed unrealistic behaviour when co-digesting lipids, since the the methane production was constant with an increasing load of X_{li} above reported LCFA inhibition thresholds (Cirne *et al.*, 2006; Astals *et al.*, 2014). LCFA is demonstrated to inhibit mainly uptake of S_{ac} (Zonta *et al.*, 2013). Therefore, a function for LCFA inhibition (I_{fa}), i.e. inhibition of uptake of S_{ac} by S_{fa}, was implemented. A Gaussian function developed and tested at the University of Queensland, Eq. (15) with two parameters, $K_{I,fa,low}$ and $K_{I,fa,high}$, was identified to best fit the observed behaviour. This function has a number of advantages over existing models (Zonta *et al.*, 2013; Palatsi *et al*., 2010), including non-competitive inhibition for threshold style inhibition. It has previously been used in the ADM1 for pH inhibition (Batstone *et al.*, 2002). The structure of the inhibition function allows explicit determination of the onset of inhibition, the point at which inhibition is full, and around a 50% inhibition point ($K_{I,50}$), which is half way between the upper and lower limits. This is important when inhibition can be complete, such as for inhibition by fats.

$$I_{fa} := \begin{cases} e^{-2.77259((S_{fa}-K_{I,fa,low})/(K_{I,fa,high}-K_{I,fa,low}))^2} & \text{for } S_{fa} > K_{I,fa,low} \\ 1 & \text{for } S_{fa} \leq K_{I,fa,low} \end{cases} \quad (15)$$

The simulation of the DAF sludge BMP test (Sections 2.4 and 3.1) revealed that I_{fa} led to a rapid acidification of the reactor with sequential pH inhibition. To describe a recovery in accordance with the measured data the lower limit of pH inhibition of uptake of acetate $pH_{LL,ac}$ was adjusted from 6 to 5 (Latif *et al*., 2015).

2.3 Plant-wide implementation of AcoD in BSM2

The GISCOD model (separate fraction/hydrolysis) was chosen for implementing AcoD in BSM2; firstly because characterisation and parameter estimation is performed independently for each substrate and secondly because it uses the same formulation of AD feed as BSM2, fractionating particulate COD as X_{ch}, X_{pr}, X_{li} and X_I rather than X_c. The later omits the disintegration step for

239 substrates and assumes a hydrolysis of each particulate COD compound as the limiting step. The
240 original interface by Nopens *et al.* (2009) from ADM1 to Activated Sludge Model No. 1 (ASM1) was
241 kept and the interface output was fed to a hydrolysis model for sludge. The co-substrates were
242 characterized and fractionated using the proposed input model and fed to separate hydrolysis model
243 blocks (Figure 2). Due to the virtual separation of hydrolysis in GISCOD it was necessary to ensure
244 that all processes were only active in the intended model reactor. To assure separation of hydrolysis
245 and remaining reactions the residual particulate substrate after hydrolysis was bypassed the ADM1
246 reactor and put back before the ADM1 to ASM1 interface.
247
248
249 Figure 2. Model layout in Simulink for the BSM2 AD block with integrated GISCOD model for AcoD.

250 ## 2.4 Case study on BMP tests and plant-wide assessment of AcoD

251 Three substrates were selected for a case study. For realism and diversity three fractions of
252 slaughterhouse waste were used: paunch, blood and dissolved air flotation (DAF) sludge, each rich on
253 carbohydrates, protein and lipids respectively. These are representative of common co-digestion feeds,
254 and in particular, the high oil and grease content of the DAF sludge means it is representative of, and
255 similar to other commonly used FOG wastes, such as grease trap waste. Analysis of these three
256 substrates is provided in Astals *et al.* (2014), and the pure substrate curves were taken from that paper,
257 where information about substrates, analytical methods and data is presented. The data used in this
258 study are given in the Supplementary information, Table S.3. The substrates were characterized using
259 the proposed input model (Section 2.1) and the BMP tests of Astals *et al.* (2014) were simulated using
260 the full ADM1. Machine fitting of parameters were performed with a least squares curve fitting
261 function for non-linear problems, `lscurvefit`, in the Matlab software package (MATLAB 8.4, The
262 MathWorks Inc., Natick, MA, USA 2014). For all substrates k_{hyd} and f_d were estimated and for DAF
263 sludge also the LCFA-inhibition parameters of Equation (15). To establish initial conditions for the
264 BMP, the standard BSM2 was run to steady state with the AD hydrolysis rate, k_{hyd}, equal to 0.3 d^{-1} and
265 biomass composition from this steady state used as inoculum composition. It should be noted that the

actual inoculum used in this study (Luggage Pt WWTP in Brisbane, QLD Australia) has a configuration very similar to the BSM2.

A plant-wide simulation study was conducted to test the developed method for modelling AcoD at WWTPs and assess the plant-wide effects of AcoD. The WWTP in the simulation study was the standard plant set-up in BSM2. The plant contains a primary clarifier, an activated sludge unit (ASU) in a Modified Ludzack-Ettinger configuration with two anoxic tanks followed by three aerobic tanks. The last aerobic tank and the first anoxic are connected by internal recycle. A secondary clarifier with sludge recycle follows the ASU. The plant sludge train contains a thickener, an AD, a co-generation unit, a dewatering unit and a storage tank. The plant layout can be found in Supplementary information, Figure S.1. The plant was simulated with the default closed loop control strategy including dissolved oxygen (DO) control in the ASU based on feed-back control of the DO in the second aerated tank (set-point 2 g $O_2.m^{-3}$) and proportional airflow rate to tanks 3 and 5. The waste activated sludge flow was set constant with seasonal values of 450 $m^3.d^{-1}$ during summer and 300 $m^3.d^{-1}$ in winter, resulting in an average sludge age of 16 days in the ASU. In the evaluation procedure two indices are calculated: (i) effluent quality index (EQI), a weighted index of the effluent quality including total suspended solids (TSS), chemical oxygen demand (COD), biological oxygen demand (BOD), total Kjeldahl nitrogen (TKN) and total nitrate and nitrite nitrogen (NOx-N); and, (ii) operational cost index (OCI) incorporating the major operational costs for aeration, pumping, mixing, sludge production and disposal, carbon source, heating of the AD and revenue from selling produced power. Plant layout, dimensions and sub-model descriptions are detailed in Gernaey *et al*. (2014).

Co-digestion feed consisted of paunch, blood and DAF sludge based on characterisation from the BMPs. A $k_{hyd,sludge}$ = 0.32 d^{-1} was applied based on Arnell and Åmand (2014). The external substrate load was calculated based on the average sludge load (organic loading rate, OLR_{sludge}), OLR_{sludge} = 2.38 kg $COD.m^{-3}.d^{-1}$, such that the base organic load of co-substrate (OLR_{ext}) was about 50% of the average sludge load: 20 $m^3.d^{-1}$ of paunch, 4 $m^3.d^{-1}$ of blood and 1 $m^3.d^{-1}$ of DAF sludge give an OLR_{ext} = 1.25 kg $COD.m^{-3}.d^{-1}$. On top of that two periods of further increased load were added; from day 350

to 410 the load of blood was increased to 15 $m^3.d^{-1}$ giving a total co-substrate OLR_{ext} of 2.11 kg $COD.m^{-3}.d^{-1}$, and from day 500 to 521 the load of DAF sludge was increased to 8 $m^3.d^{-1}$ giving a total co-substrate OLR_{ext} = 3.41 kg $COD.m^{-3}.d^{-1}$.

A full 609 days dynamic closed loop BSM2 simulation (modified with the co-digestion feed) was performed and evaluated according to the standard procedures described in Gernaey *et al.* (2014). During simulation nothing but the digester feed was changed in the default BSM2 closed loop strategy.

2.5 Input model sensitivity analysis

Many of the ADM1 state variables are not relevant or important for input fractionation, particularly when assessing plant-wide effects at WWTPs (Solon *et al.*, 2015). To assess the most influential variables in co-substrate composition a sensitivity analysis was performed using Monte Carlo simulations. The simulations were designed according to Batstone (2013) with 3 000 simulations of the BSM2 AD block. To the average sludge load of 2.4 kg $COD.m^{-3}.d^{-1}$ from BSM2 an additional 8.4 kg $COD.m^{-3}.d^{-1}$ of co-substrate was added with varying composition fractions (between 0 and 1) of X_{ch}, X_{pr} and X_{li} out of biodegradable COD. This high co-substrate load was intended to stress the digester stability and to reveal the sensitivity for different feed characteristics. Also the influence of f_d and the fraction of COD_s out of COD_t were investigated in this way. The results were evaluated with weighted principal component analysis (PCA) on the outputs gas flow (Q_{gas}), methane flow (Q_{CH4}), inorganic nitrogen (S_{IN}), pH and volatile fatty acids (VFA). Detailed information on the set-up of the Monte Carlo simulations is presented in the Supplementary information.

3 Results and Discussion

3.1 Input model case study on BMP tests

Applying the input model to the three substrates paunch, blood and DAF sludge resulted in the state variables and parameter estimates given in Table 1. The simulated and measured BMP profiles are

shown in Figure 3. The fit to data is good for paunch and blood and . While the fit to data is less accurate for DAF sludge, the model captures the main process impacts due to LCFA inhibition The ability of the process to separately identify the two parameters in the applied for I_{fa}, and its ability to simulate the complex methane production profile justify its use over simpler models, such as non-competitive inhibition. The inhibition constants estimated from DAF sludge were also used for the simulations of the other substrates. The full list of ADM1 parameter values for the BMP model is given in the Supplementary information, Table S.4.

Table 1. Resulting characterisation and parameter estimation for paunch, blood and DAF sludge. State variables not listed in the table are set to 0.

	Paunch	**Blood**	**DAF**
S_I [kg COD.m^{-3}]	0.366	0.0162	1.84E-05
S_{su} [kg COD.m^{-3}]	0.873	0.0575	0.116
S_{aa} [kg COD.m^{-3}]	0.192	0.191	0.0490
S_{fa} [kg COD.m^{-3}]	0.207	0.00540	2.83
S_{va} [kg COD.m^{-3}]	0.0612	0.102	0.0408
S_{bu} [kg COD.m^{-3}]	0.145	0.273	0.0182
S_{pro} [kg COD.m^{-3}]	0.272	0.288	0.409
S_{ac} [kg COD.m^{-3}]	0.384	1.57	0.235
S_{IN} [kmol N.m^{-3}]	0.0102	0.0279	0.00350
X_I [kg COD.m^{-3}]	15.2	1.70	0.00522
X_{ch} [kg COD.m^{-3}]	60.7	59.4	40.7
X_{pr} [kg COD.m^{-3}]	13.3	197	17.1
X_{li} [kg COD.m^{-3}]	14.4	5.58	991
k_{hyd} [d^{-1}]	0.125	0.310	0.103
B_0 [m^3 CH_4.ton VS^{-1}]	299	520	1 044
f_d [-]	0.85	0.99	1.0

$K_{I,fa,low}$ [kg COD.m^{-3}]	---*	---*	0.406
$K_{I,fa,high}$ [kg COD.m^{-3}]	---*	---*	0.714

329 * parameters not estimated for this co-substrate.

330 Figure 3. BMP curves for paunch, blood and DAF sludge. Markers represent data and lines simulation results.

331 3.2 Plant-wide assessment of AcoD

332 Figure 4 shows the organic loading rate together with the resulting total methane production and
333 relevant inhibitions. Table 2 shows the plant evaluation outputs significantly affected by AcoD as well
334 as the default BSM2 outputs, i.e. without AcoD. The addition, the co-substrates had a positive effect
335 on the methane production allowing a reduction in the overall Operational Cost Index (OCI) from 11
336 630 to 10 490. However, at the same time the effluent water quality deteriorated from the increased
337 nitrogen load in the water train, due to AD supernatant recirculation, increasing the Effluent Quality
338 Index (EQI) from 5 330 to 5 970.

339 Table 2. Evaluation results from the simulation study compared to BSM2 default values.

	BSM2 default	**BSM2 w. AcoD**
Operational Cost Index [-]	11 600	10 500
Effluent Quality Index [-]	5 330	5 970
Average aeration energy [kWh.d^{-1}]	4 130	4 380
Methane production [kg CH_4.d^{-1}]	935	1 800
Sludge production [kg SS.d^{-1}]	3 480	4 730
Effluent S_{NH} [g.m^{-3}]	0.49	0.44
Effluent S_{NO} [g.m^{-3}]	9.81	12.9
Effluent TN [g.m^{-3}]	12.3	15.4
Time in violation TN [%]	0.17	15.0

340

The reduction in OCI corresponds to a total reduction of the operational costs for the WWTP by 10%. This significant reduction was achieved because the revenue from selling co-generated power from the produced methane increased by 92%; although both the aeration energy index and the sludge production at the same time increased by 6 and 39%, respectively. Following the BSM2 evaluation procedure neither the transport cost nor gate fee revenue of the co-substrate is included in the evaluation (Malmqvist *et al.*, 2006). In the dynamic profiles of Figure 4 the effect of the two short-term load increases of blood and DAF sludge can be seen. The increased load of blood did not yield a proportional increase in methane production. This is because the elevated ammonia levels in the AD at the same time cause a more severe ammonia inhibition in the model. In contrast, the load peak of DAF sludge increased the methane production proportional to the load, since LCFA was minor under this scenario

Figure 4. Effect of AcoD on BSM2 AD process. Methane production (top), OLR (second), ammonia inhibition (I_{NH}, third) and LCFA inhibition (I_{fa}, bottom). Grey lines are standard BSM2 results without AcoD and black lines are the simulated scenario with AcoD (filtered values).

The increase in EQI was mainly due to a higher effluent total nitrogen (TN), 15.4 g N.m^{-3} caused by the nitrogen load from the protein rich co-substrate, which elevated the S_{NH} concentration in the returning AD supernatant; from an average of 1 290 g N.m^{-3} to 1 610 g N.m^{-3} (Figure 5). This led to a time in violation of the effluent constrains for TN of 15% compared to 0.17% without AcoD. The violation of the effluent constrains would be an unacceptable effect of AcoD and shows the importance of selection and dose strategy for the co-substrate. The primary cause of high effluent TN was elevated effluent S_{NO} caused by insufficient carbon availability for denitrification rather than poor nitrification (Table 2, Figure 5). The reason for this is that the default control strategy of the closed loop BSM2 has a DO control in the ASU responding to the increased ammonia load but only a fixed dosage of methanol. If the same total load of blood would have dosed over the whole period the methanol scarcity might had been less pronounced, or if it had been dosed for an even shorter period

the nitrification capacity would have been exceeded as well. Effluent limit violation would have been avoided simulating an increased or controlled methanol dosage. The draw-back of the increased nitrogen load would then have manifested itself as increased methanol consumption instead of effluent violation. While being outside the scope of this publication, the strategies to cope with increased nitrogen load can easily be tested and evaluated with additional simulations (results not shown). This demonstrates how simulating AcoD in plant-wide WWTP models allows to design an optimal co-substrate composition and feed strategy and simultaneously control the effects on the water train. The presented simulation study shows the applicability of modelling and simulation to assess cost-benefit and the plant-wide effects of AcoD on WWTPs.

Figure 5. Effect of AcoD on S_{NH} in dewatering supernatant (top) and S_{NO} in plant effluent (bottom). Grey lines are standard BSM2 results without AcoD and black lines are the simulated scenario with AcoD (filtered values).

3.3 Influent sensitivity analysis

The simulations varying co-substrate biodegradability (f_d) confirm that the feed degradable COD fraction is very important, as previously shown (Solon *et al.*, 2015; Galí *et al.*, 2009). The resulting PCA of the Monte Carlo simulations from varying X_{ch}, X_{pr} and X_{li} is shown in Figure 6 (additional figures of model outputs related to feed composition can be found in the Supplementary information, Figures S.3 and S.4). The variations in the results are explained to 71.5% by Component 1 and 25.2% by Component 2. The variation in Component 1 is positively related to biogas and methane flow and negatively to VFA. Component 2 is mostly influenced by the S_{IN} concentration in the effluent digestate. Three distinctive regions can be seen marked in Figure 6:

I. the substrate compositions positive in Component 1 and negative in Component 2 represent a well-functioning digester with low VFAs and good methane production;
II. as the protein content increases the output gradually moves from region I into II, i.e. negative in Component 1 but positive in Component 2, towards the upper-left corner. This

substrate composition is at or close to digester failure as the ammonia inhibition is gradually increasing along with VFAs leading to decreasing methane production;

III. the clustered samples negative in both Components 1 and 2 are all high in X_{li} and represent the very disruptive digester failure due to LCFA inhibition where methane production totally stops and VFA increases dramatically leading to total pH inhibition. There is a relatively rapid switch from region I to region III due to the threshold nature of inhibition, specifically, when 58% of the co-substrate load of 8.4 kg COD.m^{-3}.d^{-1} consists of X_{li}.

This leads to the conclusion that apart from f_d, the two most important input model parameters for digester stability with co-digestion are fractions determining X_{pr} and X_{li}. The results also show that X_{ch} is relevant for the total gas production (Figure S.3 in the Supplementary information) because a higher X_{ch} fraction leads to increased CO_2 production; which is coherent with Solon *et al.* (2015). Moreover, Figure S.3 reveals that high loads of carbohydrates will lead to pH inhibition subsequent to high VFA production.

Figure 6. Principal Component Analysis for the Monte Carlo simulations with varying AD feed composition.

4 Conclusions

Anaerobic co-digestion was for the first time implemented in BSM2, The GISCOD model was used to model AcoD complemented by a Gaussian LCFA inhibition function.

- A new input model for fractionation of COD was developed based on feasible and affordable tests. The method was proven reliable based on modelling of BMP tests of three substrates paunch, blood and DAF sludge.

ACCEPTED MANUSCRIPT

- A performance assessment study of AcoD was performed with a dynamic feed mix. It revealed that the overall operational cost was reduced by 10%. However, the high nitrogen content in blood increased ammonia inhibition in the digester, leading to lower digester performance, and overloaded the denitrification capacity of the water train and deteriorated the effluent water quality.
- A sensitivity analysis on co-substrate feed characteristics found that apart from the biodegradable fraction of COD, protein and lipid fractions of particulate biodegradable COD were the two most important state variables for digester stability and methane production, and that different substrates caused different modes of failure.

5 Acknowledgements

The authors acknowledge the financial support obtained through the Swedish Research Council Formas (211-2010-141), the Swedish Water & Wastewater Association (10-106), SP Technical Research Institute of Sweden and the Swedish research and education consortium VA-cluster Mälardalen.

ACCEPTED MANUSCRIPT

ACCEPTED MANUSCRIPT

6 References

Angelidaki, I., Alves, M., Bolzonella, D., Borzacconi, L., Campos, J.L., Guwy, A.J., Kalyuzhnyi, S., Jenicek, P. and van Lier, J.B. (2009) Defining the biomethane potential (BMP) of solid organic wastes and energy crops: a proposed protocol for batch assays. Water Science and Technology, 59(5), 927-934.

Arnell, M. and Åmand, L. (2014) Parameter estimation for modelling of anaerobic co-digestion. IWA 9th World Water Congress and Exhibition (IWA2014), Lisbon, Portugal, 21-26 September, 2014.

Astals, S., Batstone, D.J., Mata-Alvarez, J. and Jensen, P.D. (2014) Identification of synergistic impacts during anaerobic co-digestion of organic wastes. Bioresource Technology, 169, 421-427.

Astals, S., Esteban-Gutiérrez, M., Fernández-Arévalo, T., Aymerich, E., García-Heras, J.L. and Mata-Alvarez, J. (2013) Anaerobic digestion of seven different sewage sludges: A biodegradability and modelling study. Water Research, 47(16), 6033-6043.

Batstone, D.J., Keller, J., Angelidaki, R.I., Kalyuzhnyi, S.V., Pavlostathis, S.G., Rozzi, A., Sanders, W.T.M., Siegrist, H. and Vavilin, V.A. (2002) Anaerobic Digestion Model No. 1. Scientific and Technical Report No. 13, IWA Publishing, London, UK.

Batstone, D.J. (2013) Teaching uncertainty propagation as a corecomponent in process engineering statistics. Education for Chemical Engineers, 8, 132–139.

Batstone, D. J., and Virdis, B. (2014) The role of anaerobic digestion in the emerging energy economy. Current Opinion in Biotechnology, 27, 142-149.

459 Batstone, D.J., Puyol, D., Flores-Alsina, X. and Rodríguez, J. (2015) Mathematical modelling of
460 anaerobic digestion processes: applications and future needs. Reviews in Environmental Science and
461 Biotechnology, 14(4), 595-613.
462
463 Cirne, D.G., Paloumet, X., Björnsson, L., Alves, M.M. and Mattiasson, B. (2007) Anaerobic digestion
464 of lipid-rich waste - Effects of lipid concentration. Renewable Energy, 32, 965-975.
465
466 Derbal, K., Bencheikh-Lehocine, M., Cecchi, F., Meniai, A.-H. and Pavan, P. (2009) Application of
467 the IWA ADM1 model to simulate anaerobic co-digestion of organic waste with waste activated
468 sludge in mesophilic condition. Bioresource Technology, 100, 1539-1543.
469
470 Esposito, G., Frunzo, L., Panico, A. and d'Antonio, G. (2008) Mathematical modelling of
471 disintegration-limited co-digestion of OFMSW and sewage sludge. Water Science and Technology,
472 58(7), 1513-1519.
473
474 Galí, A., Benabdallah, T., Astals, S. and Mata-Alvarez, J. (2009) Modified version of ADM1 model
475 for agro-waste application. Bioresource Technology, 100, 2783-2790.
476
477 Garcia-Gen, S., Lema, J.M. and Rodriguez, J. (2013) Generalised modelling approach for anaerobic
478 co-digestion of fermentable substrates. Bioresource Technology, 147, 525-533.
479
480 Gernaey, K., Jeppsson, U., Vanrolleghem, P.A. and Copp, J.B. (2014) Benchmarking of Control
481 Strategies for Wastewater Treatment Plants. IWA Scientific and Technical Report No. 23. IWA
482 Publishing, London, UK.
483
484 Girault, R., Bridoux, G., Nauleau, F., Poullain, C., Buffet, J., Steyer, J.P., Sadowski, A.G. and Béline,
485 F. (2012) A waste characterisation procedure for ADM1 implementation based on degradation
486 kinetics. Water Research, 46(13), 4099-4110.

ACCEPTED MANUSCRIPT

Jensen, P.D., Ge, H. and Batstone, D.J. (2011) Assessing the role of biochemical methane potential tests in determining anaerobic degradability rate and extent. Water Science and Technology, 64(4), 880-886.

Jimenez, J., Aemig, Q., Doussiet, N., Steyer, J.P., Houot, S. and Patureau, D. (2015) A new organic matter fractionation methodology for organic wastes: Bioaccessibility and complexity characterization for treatment optimization. Bioresource Technology, 194, 344-353.

Kleerebezem, R. and van Loosdrecht, M.C.M. (2006) Waste characterization for implementation in ADM1. Water Science and Technology, 54(4), 157-174.

Latif, M.A., Mehta, C.M. and Batstone, D.J. (2015) Low pH anaerobic digestion of waste activated sludge for enhanced phosphorous release. Water Research, 81, 288-293.

Lundkvist, M. (2005) Energieffektivisering (Sweco report 2005-01-14T) [in Swedish]. Sweco, Halmstad, Sweden.

Lübken, M., Wichern, M., Schlattmann, M., Gronauer, A. and Horn, H. (2007) Modelling the energy balance of an anaerobic digester fed with cattle manure and renewable energy crops. Water Research, 41(18), 4085-4096.

Malmqvist, P.A., Heinicke, G., Kärrman, E., Stenström, T.A. and Svensson, G. (2006) Strategic Planning of Sustainable Urban Water Management. IWA Publishing, London, UK.

Mata-Alvarez, J., Dosta, J., Romero-Güiza, M.S., Fonoll, X., Peces, M. and Astals, S. (2014) A critical review on anaerobic co-digestion achievements between 2010 and 2013. Renewable and Sustainable Energy Reviews, 36, 412-427.

Nopens, I., Batstone, D., Copp, J.B., Jeppsson, U., Volcke, E.I.P., Alex, J. and Vanrolleghem, P.A. (2009) An ASM/ADM model interface for dynamic plant-wide simulation. Water Research, 43(7), 1913-1923.

Olsson G. (2015) Water and Energy: Threats and Opportunities - Second Edition. IWA Publishing, London, UK.

Palatsi, J., Illa, J., Prenafeta-Boldú, F.X., Laureni, M., Fernandez, B., Angelidaki, I. and Flotats, X. (2010) Long-chain fatty acids inhibition and adaptation process in anaerobic thermophilic digestion: Batch tests, microbial community structure and mathematical modelling. Bioresource Technology, 101(7), 2243-2251.

Razaviarani, V. and Buchanan, I.D. (2015) Calibration of the Anaerobic Digestion Model No. 1 (ADM1) for steady-state anaerobic co-digestion of municipal wastewater sludge with restaurant grease trap waste. Chemical Engineering Journal, 266, 91-99.

Solon, K., Flores-Alsina, X., Gernaey, K.V. and Jeppsson, U. (2015) Effects of influent fractionation, kinetics, stoichiometry and mass transfer on CH4, H2 and CO2 production for (plant-wide) modeling of anaerobic digesters. Water Science and Technology, 71(6), 870-877.

Wichern, M., Gehring, T., Fischer, K., Andrade, D., Lübken, M., Koch, K., Gronauer, A. and Horn, H. (2009) Monofermentation of grass silage under mesophilic conditions: measurements and mathematical modelling with ADM1. Bioresource Technology, 100(4), 1675-1681.

Zaher, U., Li, R., Jeppsson, U., Steyer, J.P. and Chen, S. (2009) GISCOD: General Integrated Solid waste Co-Digestion model. Water Research, 43(10), 2717-2727.

ACCEPTED MANUSCRIPT

543 Zonta, Z., Alves, M.M., Flotats, X. and Palatsi, J. (2013) Modelling inhibitory effects of long chain

544 fatty acids in the anaerobic digestion process. Water Research, 47(3), 1369-1380.

545

ACCEPTED MANUSCRIP

Supplementary information

Benchmark Simulation Model No.2 plant layout

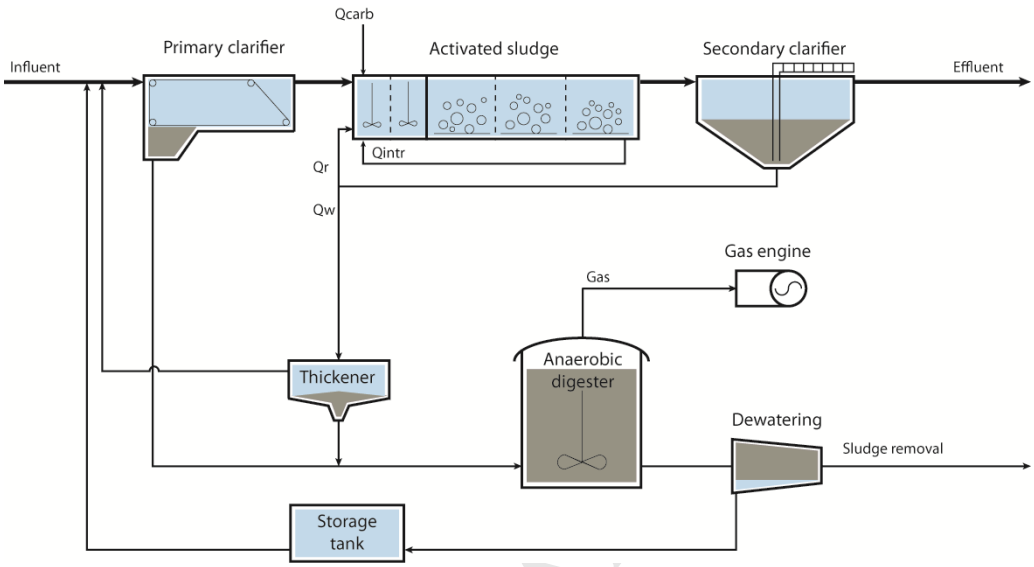

Figure S.1. Plant layout for the wastewater treatment plant in Benchmark Simulation Model No. 2 (Gernaey *et al.*, 2014).

ADM1 state variables

Table S.1. State variables of ADM1 (Batstone *et al.*, 2002). *S* denotes solubles and *X* particulates.

State variable	Description	State variable	Description
S_{su}	monosaccharides	X_c	composite
S_{aa}	amino acids	X_{ch}	carbohydrates
S_{fa}	total LCFA	X_{pr}	proteins
S_{va}	total valerate	X_{li}	lipids
S_{bu}	total butyrate	X_{su}	biomass
S_{pro}	total propionate	X_{aa}	biomass

ACCEPTED MANUSCRIPT

S_{ac}	total acetate	X_{fa}	biomass
S_{h2}	hydrogen	X_{c4}	biomass
S_{ch4}	methane	X_{pro}	biomass
S_{ic}	inorganic carbon	X_{ac}	biomass
S_{IN}	inorganic nitrogen	X_{h2}	biomass
S_{I}	soluble inerts	X_{I}	particulate inerts
S_{cat}	cations		
S_{an}	anions		

COD conversion factors

Table S.2. Conversion factors (γ) for organic fractions into COD (Grau *et al.*, 2007).

	Value
γ_{ac} [kg COD.(kg ac)$^{-1}$]	1.066667
γ_{pro} [kg COD.(kg pro)$^{-1}$]	1.513514
γ_{bu} [kg COD.(kg bu)$^{-1}$]	1.818182
γ_{va} [kg COD.(kg va)$^{-1}$]	2.039216
γ_{Pr} [kg COD.(kg Pr)$^{-1}$]	1.53
γ_{Li} [kg COD.(kg Li)$^{-1}$]	2.878

Substrate data

Table S.3. Analysis data used for substrate characterisation. From Astals *et al.* (2014) with modifications indicated.

	Paunch	Blood	DAF sludge

TS [kg.m^{-3}]	117	187	360
VS [kg.m^{-3}]	106	178	353
COD_t [kg COD.m^{-3}]	106	266	1 053
COD_s [kg COD.m^{-3}]	2.5	2.5[1]	3.7
Acetate [kg.m^{-3}]	0.36	1.47	0.22
Propionate [kg.m^{-3}]	0.18	0.19	0.27
Butyrate [kg.m^{-3}]	0.08	0.15	0.01
Valerate [kg.m^{-3}]	0.03	0.05	0.02
Proteins [kg.m^{-3}]	10.2	129.5	11.8
Lipids [kg.m^{-3}]	5.85[2]	1.95[2]	344.5[2]
TAN [g N.m^{-3}]	143	391	49

[1] measured value is higher but most COD except VFAs are assumed colloidal and therefore particulates needed to be hydrolysed;

[2] analysed values are too low due to faulty analysis and increased by 30%.

ADM1 parameters

Table S.4. Model parameters used for ADM1 in the plant-wide simulation study. Units; N_i [kmol N.(kg COD)$^{-1}$], C_i [kmol C.(kg COD)$^{-1}$], Y_i [kg COD_X.(kg COD_S)$^{-1}$], k_i (decay rates) [d^{-1}], K_S_i [kg COD_S.m^{-3}], k_m_i [kg COD_S.(kg COD_X)$^{-1}$.d^{-1}], K_I_i [kg COD.m^{-3}], k_A_Bi [M^{-1}.d^{-1}], kLa [d^{-1}], K_A_i [M], R [bar.m^{3}.kmol^{-1}.K^{-1}].

Parameter	Value	Parameter	Value	Parameter	Value
f_sI_xc	0.1	Y_aa	0.08	pH_UL_h2	6
f_xI_xc	0.2	Y_fa	0.06	pH_LL_h2	5
f_ch_xc	0.2	Y_c4	0.06	k_dec_Xsu	0.02
f_pr_xc	0.2	Y_pro	0.04	k_dec_Xaa	0.02
f_li_xc	0.3	C_ch4	0.0156	k_dec_Xfa	0.02
N_xc	0.002685714	Y_ac	0.05	k_dec_Xc4	0.02

N_I	0.004285714	Y_h2	0.06	k_dec_Xpro	0.02
N_aa	0.007	k_dis	10	k_dec_ac	0.02
C_xc	0.02786	k_hyd_ch	0.2	k_dec_h2	0.02
C_sI	0.03	k_hyd_pr	0.3	R	0.083145
C_ch	0.0313	k_hyd_li	0.1	T_op	308.15
C_pr	0.03	K_S_IN	0.0001	pK_w_base	14
C_li	0.022	k_m_su	30	pK_a_va_base	4.86
C_xI	0.03	K_S_su	0.5	pK_a_bu_base	4.82
C_su	0.0313	pH_UL_aa	5.5	pK_a_pro_base	4.88
C_aa	0.03	pH_LL_aa	4	pK_a_ac_base	4.76
f_fa_li	0.95	k_m_aa	50	pK_a_co2_base	6.35
C_fa	0.0217	K_S_aa	0.3	pK_a_IN_base	9.25
f_h2_su	0.19	k_m_fa	6	k_A_Bva	1E+10
f_bu_su	0.13	K_S_fa	0.4	k_A_Bbu	1E+10
f_pro_su	0.27	K_Ih2_fa	0.000005	k_A_Bpro	1E+10
f_ac_su	0.41	k_m_c4	20	k_A_Bac	1E+10
N_bac	0.005714286	K_S_c4	0.2	k_A_Bco2	1E+10
C_bu	0.025	K_Ih2_c4	0.00001	k_A_BIN	1E+10
C_pro	0.0268	k_m_pro	13	kLa	200
C_ac	0.0313	K_S_pro	0.1	K_H_h2o_base	0.0313
C_bac	0.0313	K_I_h2_pro	3.5E-06	K_H_co2_base	0.035
Y_su	0.1	k_m_ac	8	K_H_ch4_base	0.0014
f_h2_aa	0.06	K_S_ac	0.15	K_H_h2_base	0.00078
f_va_aa	0.23	K_I_nh3	0.0018	k_P	50 000
f_bu_aa	0.26	pH_UL_ac	7	K_I_fa_low	0.40639
f_pro_aa	0.05	pH_LL_ac	5	K_I_fa_high	0.71421
f_ac_aa	0.4	k_m_h2	35		

C_va	0.024	K_S_h2	0.000007

570

571 **Monte Carlo simulations for sensitivity analysis**

572 The Monte Carlo simulations were made in the Matlab/Simulink software package (MATLAB 8.4,
573 The MathWorks Inc., Natick, MA, 2014). The model used for the sensitivity analysis was the AD-
574 block from the Benchmark Simulation Model No. 2 (BSM2, Gernaey *et al.*, 2014) plant with a sludge
575 feed composition equal to the steady state sludge feed from BSM2. This is a simplification since the
576 sludge feed would be slightly affected by the changed composition of the recycled digester supernatant
577 if anaerobic co-digestion (AcoD) is introduced. The simulations were run for 130 days with constant
578 influent conditions.

579

580 The generation of the 3 000 co-substrate feed samples followed the description in Batstone (2013).
581 Basic data for the feed is given in Table S.1. The co-substrate normal distributed samples with varying
582 fractions of carbohydrates, proteins and lipids out of bio-degradable particulate COD (f_{ch}, f_{pr} and f_{li})
583 were generated with normalised inverted random numbers with the function call:

584 `f_i = norminv(rand(n,1),f_mean,0.2);`

585 the f_{ch} was generated with a mean, f_{mean} = 0.33 and out of the remaining part f_{pr} was generated with f_{mean}
586 = 0.5 and the residual was assigned to f_{li}. Values less than 0 or greater than 1 were set to 0 and 1,
587 respectively. The resulting influent profiles are shown in Figure S.1.

588

589 Table S.5. Basic system and feed data for the simulations.

	Co-substrate	**Sludge**
COD_t [kg.m^{-3}]	1 250	44.8
Biodegradable part of COD	0.75	0.768
Q_{feed} [m^3.d]	30	178.46

OLR [kg COD.m^{-3}.d^{-1}]	8.38	2.35

590

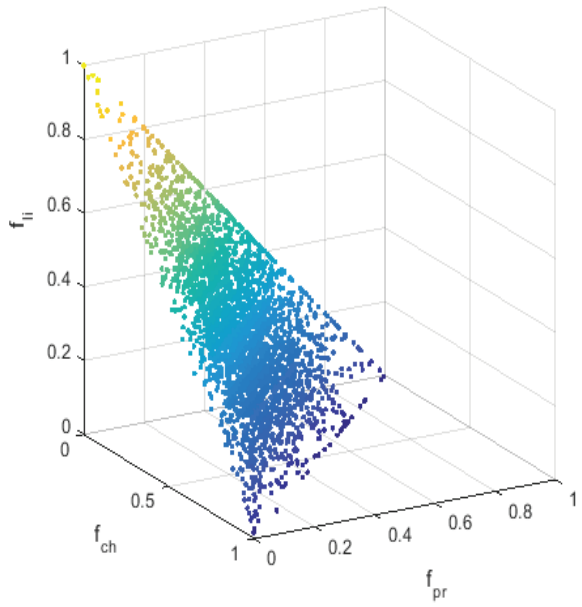

591

592 Figure S.2 Profiles of f_{ch}, f_{pr} and f_{li} for the 3 000 samples used for Monte Carlo simulations.

ACCEPTED MANUSCRIPT

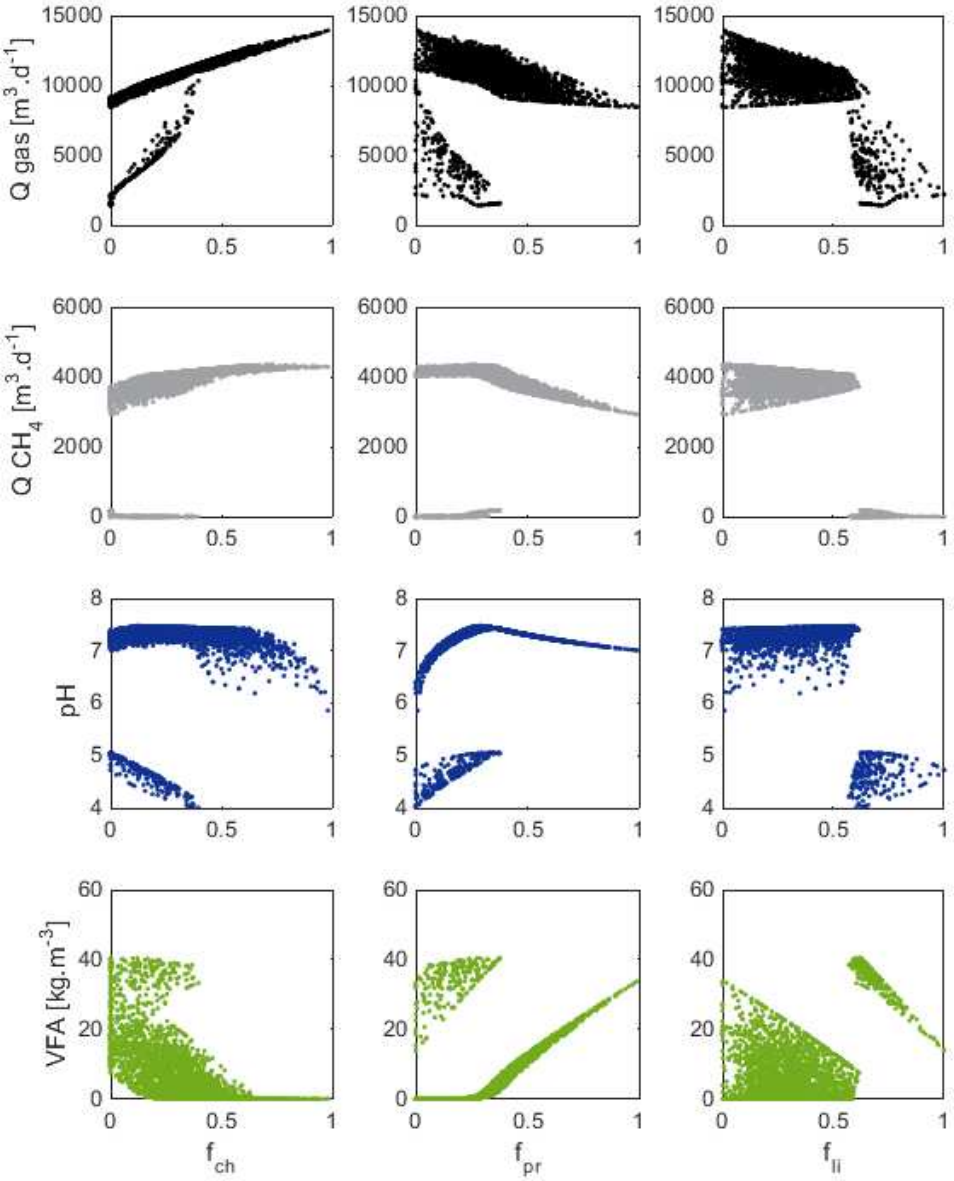

593

594 Figure S.3. Output state variables from the Monte Carlo simulations. From top to bottom the rows

595 depict, Q_{gas}, Q_{CH4}, pH and VFA. Each state variable is plotted against the fraction of carbohydrates

596 (f_{ch}), proteins (f_{pr}) and lipids (f_{li}), respectively, from left to right.

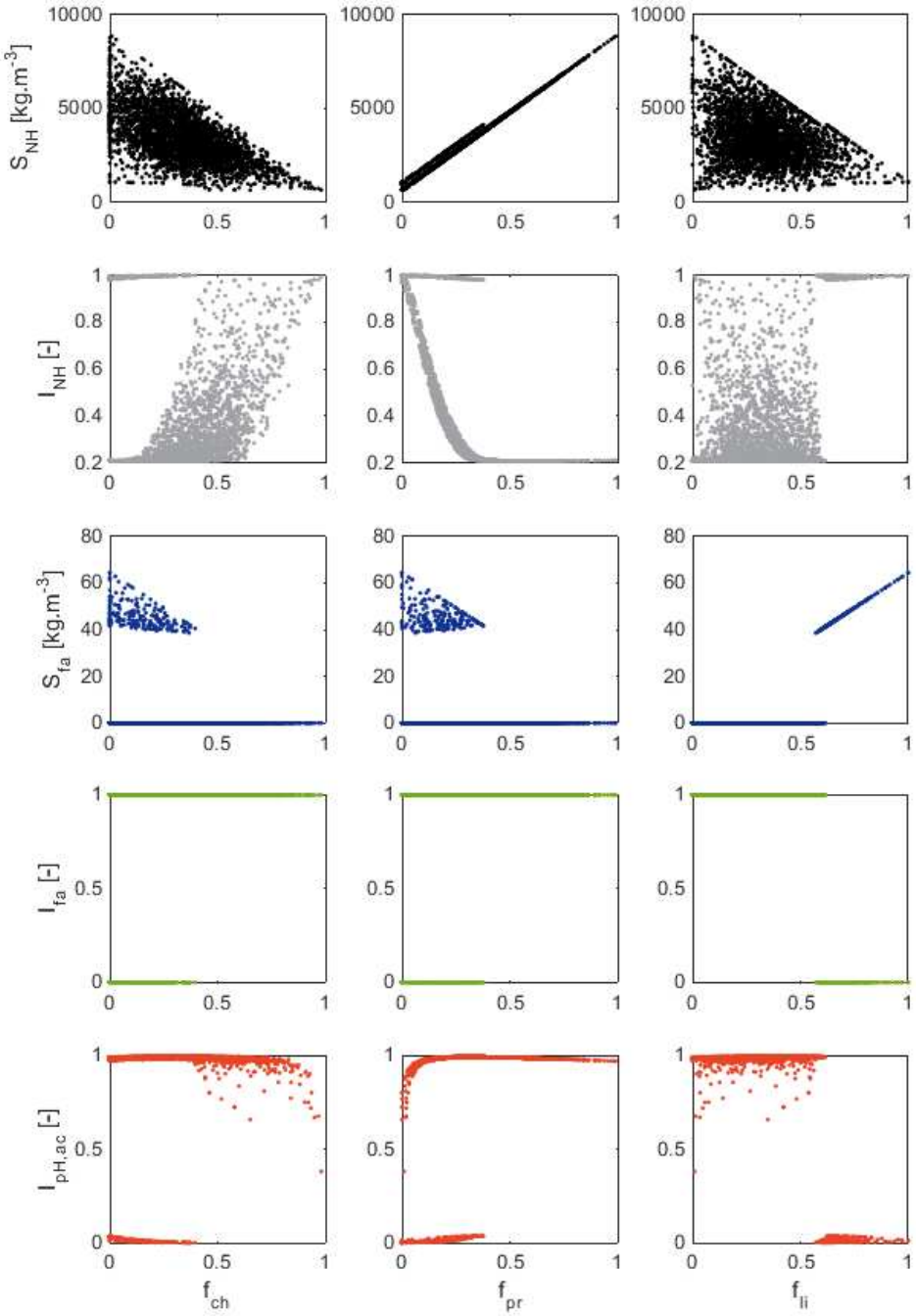

Figure S.4. AD inhibitions and corresponding inhibitory compound from the Monte Carlo simulations. From top to bottom the rows depict, S_{NH}, I_{NH}, S_{fa}, I_{fa} and $I_{pH,ac}$. Each state variable is plotted against the fraction of carbohydrates (f_{ch}), proteins (f_{pr}) and lipids (f_{li}), respectively, from left to right.

ACCEPTED MANUSCRIPT

602

603

604

605

606

607 **References**

608 Astals, S., Batstone, D.J., Mata-Alvarez, J. and Jensen, P.D. (2014) Identification of synergistic
609 impacts during anaerobic co-digestion of organic wastes. Bioresource Technology, 169, 421-427.

610

611 Batstone, D.J., Keller, J., Angelidaki, R.I., Kalyuzhnyi, S.V., Pavlostathis, S.G., Rozzi, A., Sanders,
612 W.T.M., Siegrist, H. and Vavilin, V.A. (2002) Anaerobic Digestion Model No. 1. Scientific and
613 Technical Report No. 13, IWA Publishing, London, UK.

614

615 Batstone, D.J. (2013) Teaching uncertainty propagation as a core component in process engineering
616 statistics. Education for Chemical Engineers, 8, 132-139.

617

618 Gernaey, K., Jeppsson, U., Vanrolleghem, P.A. and Copp, J.B. (2014) Benchmarking of Control
619 Strategies for Wastewater Treatment Plants. IWA Scientific and Technical Report No. 23, IWA
620 Publishing, London, UK.

621

622 Grau, P., de Gracia, M., Vanrolleghem, P.A. and Ayesa, E. (2007) A new plant-wide modelling
623 methodology for WWTPs. Water Research, 41(19), 4357-4372.

ACCEPTED MANUSCRIPT

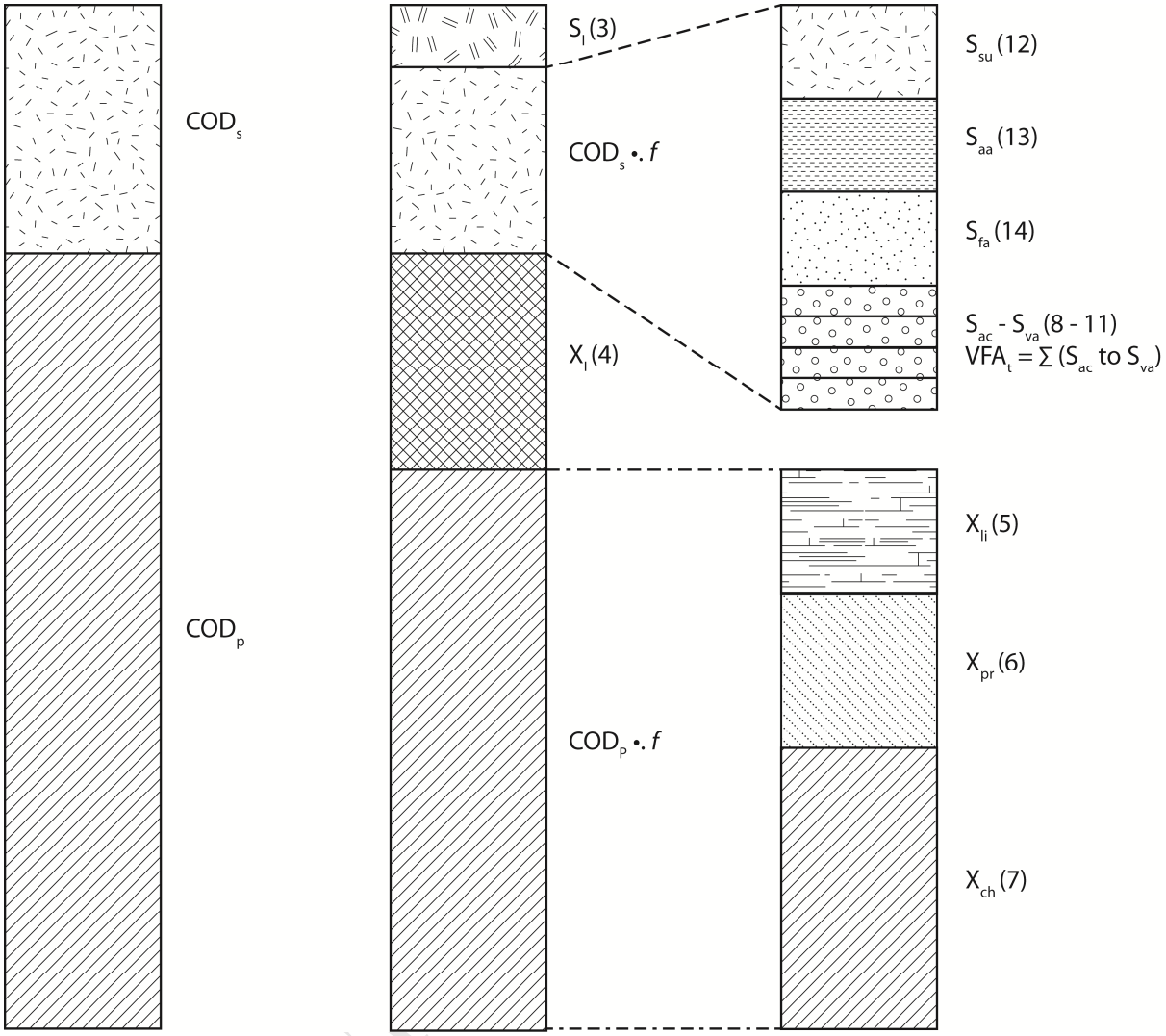

ACCEPTED MANUSCRIPT

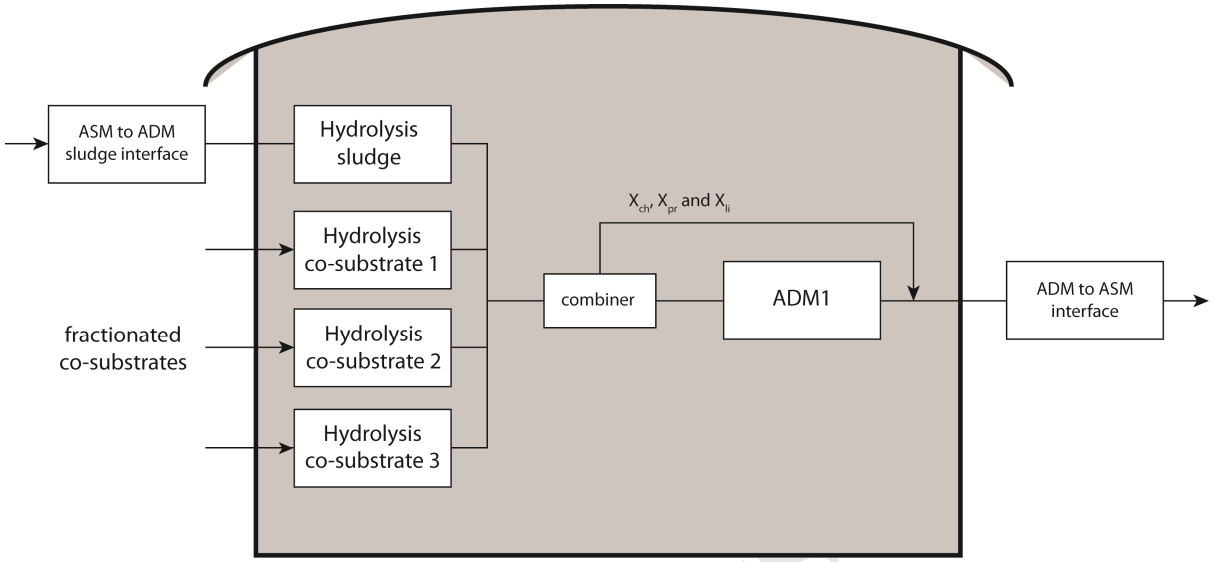

ACCEPTED MANUSCRIPT

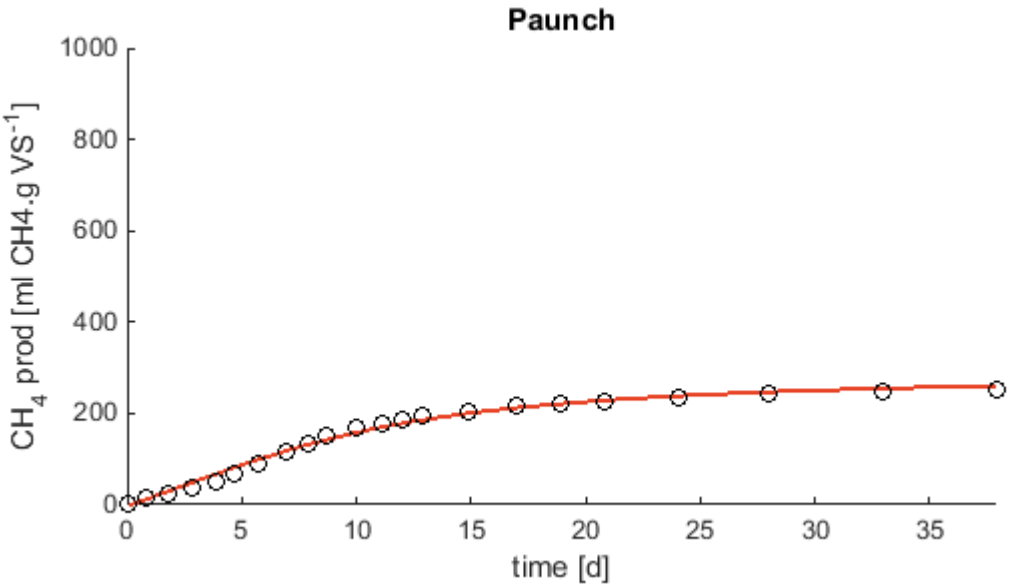

ACCEPTED MANUSCRIPT

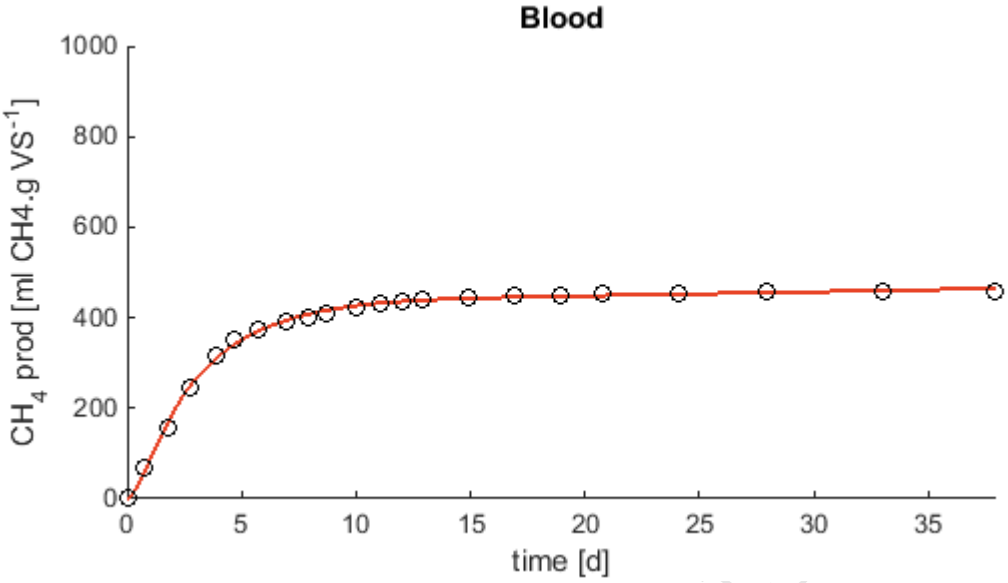

ACCEPTED MANUSCRIPT

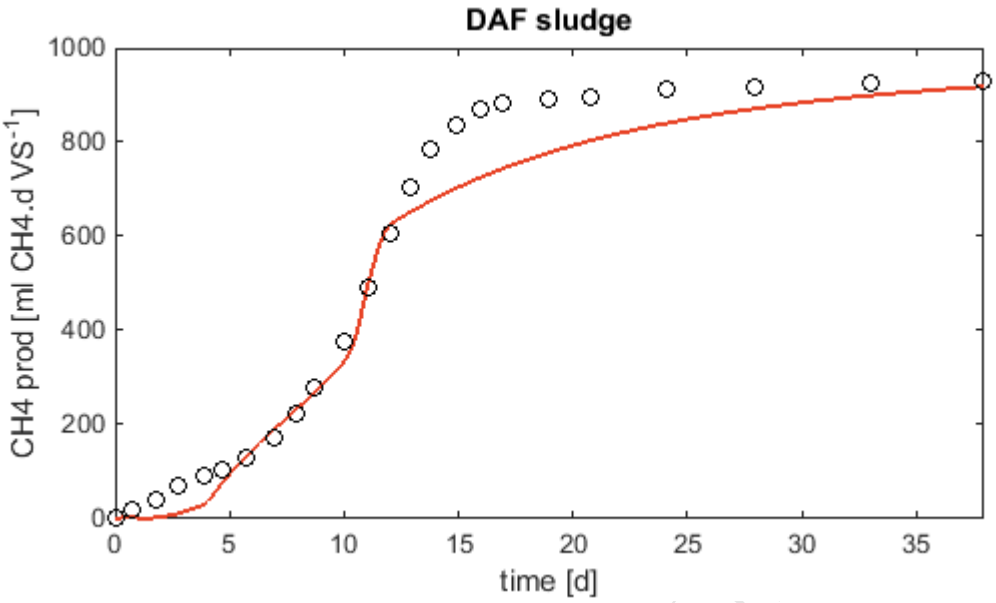

ACCEPTED MANUSCRIPT

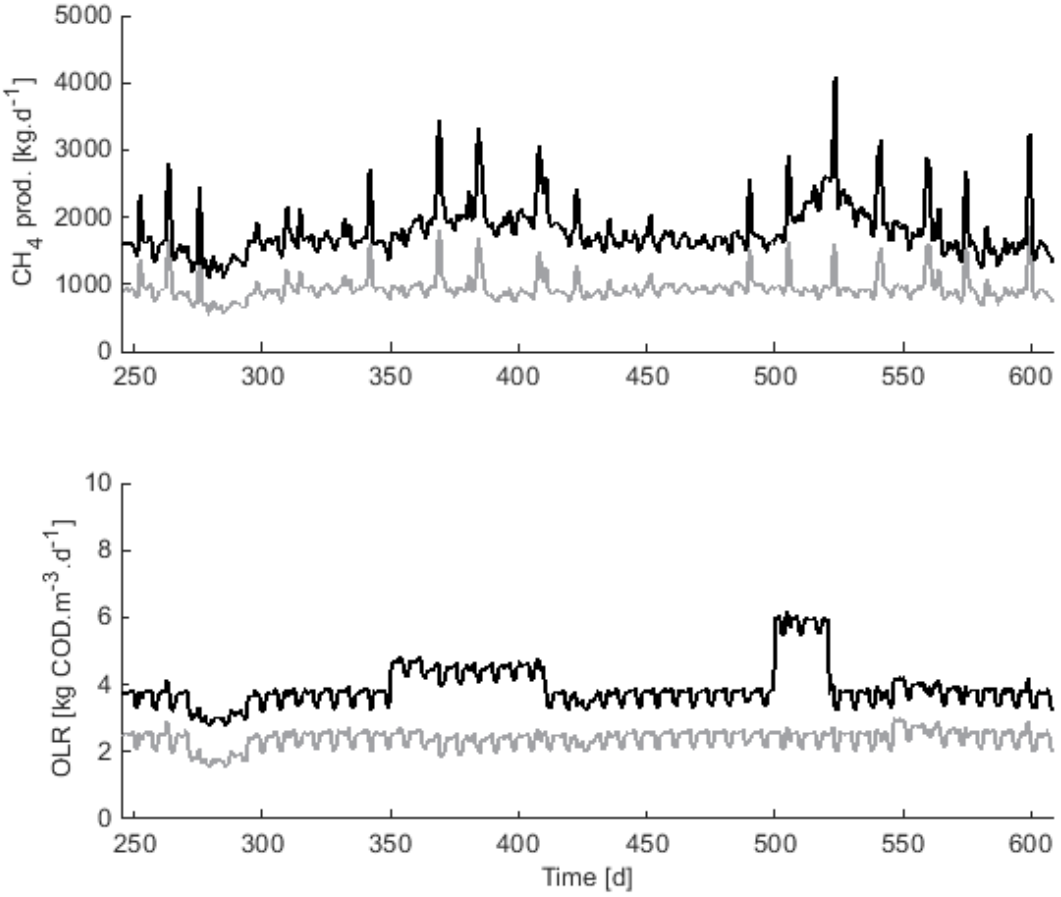
5000
4000
3000
2000
1000
0
CH_4 prod. [kg.d^{-1}]
250
300
350
400
450
500
550
600
10
8
6
4
2
0
OLR [kg COD.m^{-3}.d^{-1}]
Time [d]

ACCEPTED

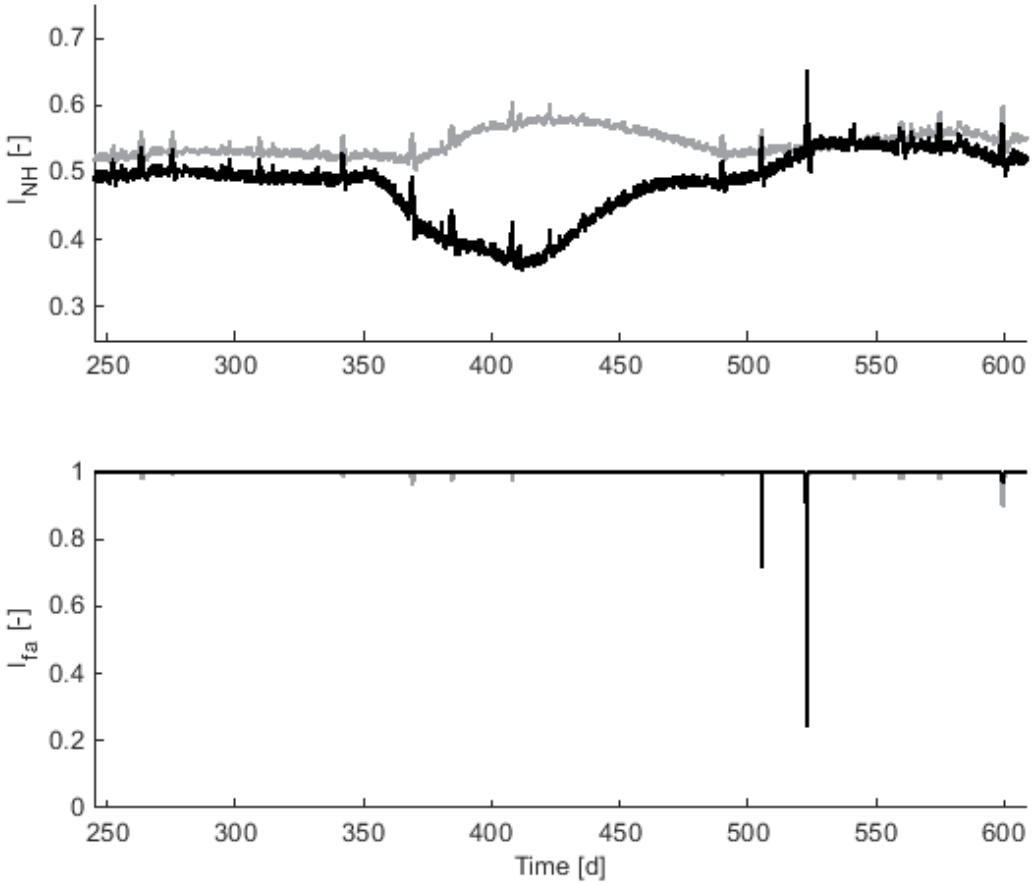
0.7
0.6
0.5
0.4
0.3
I_{NH} [-]
250
300
350
400
450
500
550
600
1
0.8
0.6
0.4
0.2
0
I_{fa} [-]
250
300
350
400
450
500
550
600
Time [d]

ACCEPTED

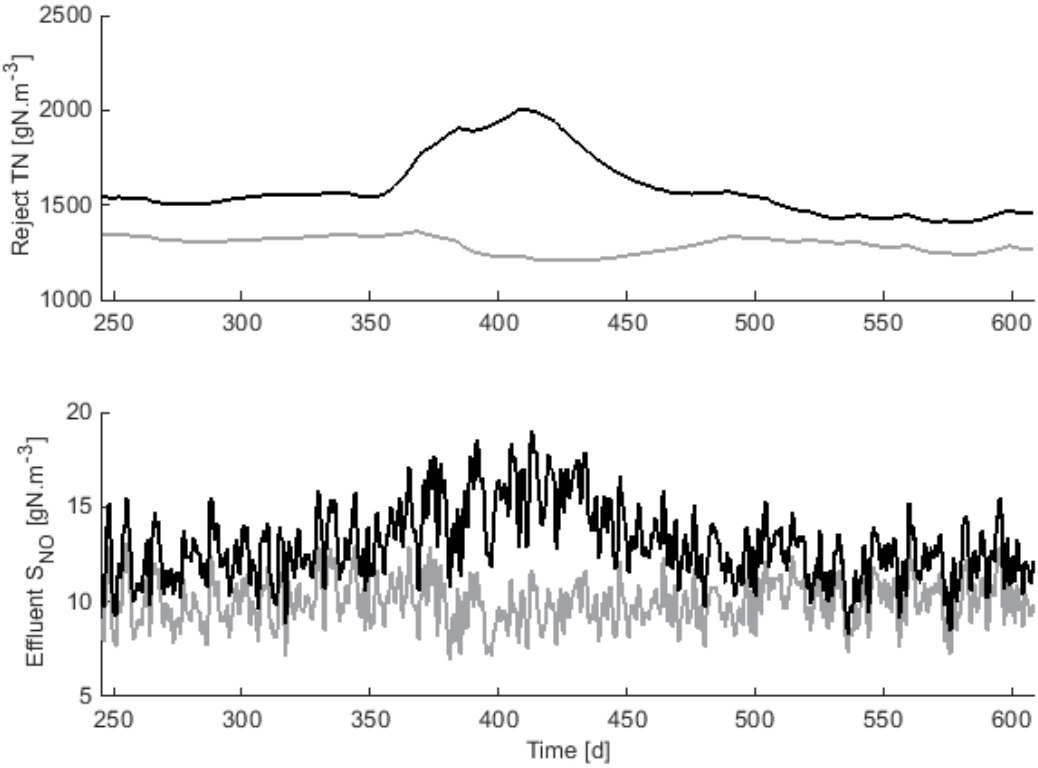

ACCEPTED MANUSCRIPT

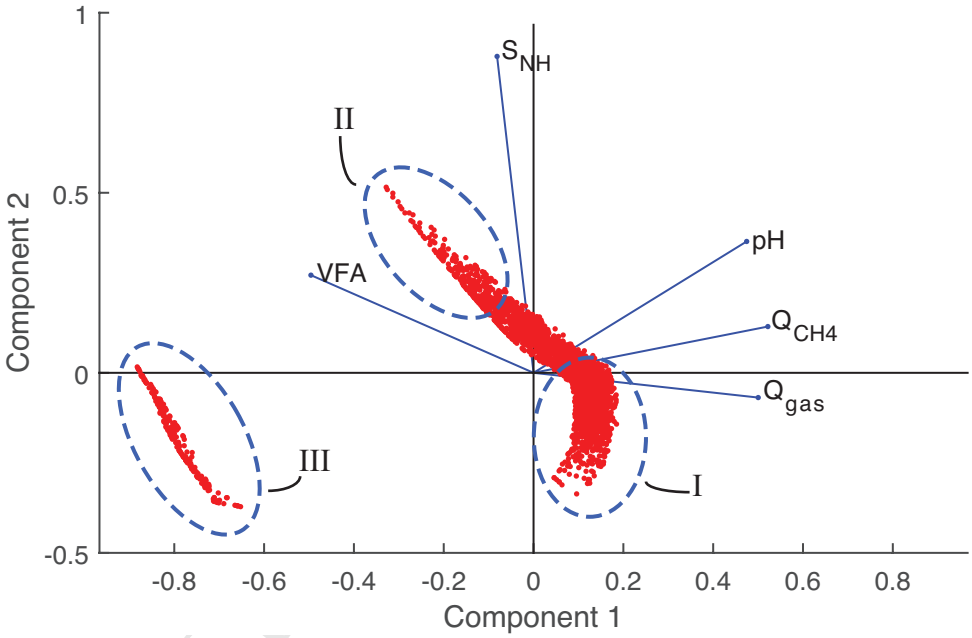

ACCEPTED MANUSCRIPT